

Constructing Bayesian Pseudo-Coresets using Contrastive Divergence

Piyush Tiwary
Indian Institute of Science
Bangalore, India
piyushtiwary@iisc.ac.in

Kumar Shubham
Indian Institute of Science
Bangalore, India
shubhamkuma3@iisc.ac.in

Vivek Kashyap
Bangalore Institute of Technology
Bangalore, India
vivekvkashyap10@gmail.com

Prathosh A.P.
Indian Institute of Science
Bangalore, India
prathosh@iisc.ac.in

Abstract

Bayesian Pseudo-Coreset (BPC) and Dataset Condensation are two parallel streams of work that construct a synthetic set such that, a model trained independently on this synthetic set, yields the same performance as training on the original training set. While dataset condensation methods use non-bayesian, heuristic ways to construct such a synthetic set, BPC methods take a bayesian approach and formulate the problem as divergence minimization between posteriors associated with original data and synthetic data. However, BPC methods generally rely on distributional assumptions on these posteriors which makes them less flexible and hinders their performance. In this work, we propose to solve these issues by modeling the posterior associated with synthetic data by an energy-based distribution. We derive a contrastive-divergence-like loss function to learn the synthetic set and show a simple and efficient way to estimate this loss. Further, we perform rigorous experiments pertaining to the proposed method. Our experiments on multiple datasets show that the proposed method not only outperforms previous BPC methods but also gives performance comparable to dataset condensation counterparts.

1. Introduction

Modern deep learning models have shown impressive performance on a variety of applications such as computer vision, natural language processing, and speech processing [1, 10, 11, 18, 29, 38]. Large training datasets and heavy computational infrastructure have played a pivotal role in achieving such performance. Moreover, the availability of large training datasets is critical to improving the performance of these models. This reliance on large datasets not only increases the computational complexity required

to train these models but also adds to the total training time required to achieve acceptable accuracy. Typically, training time for larger datasets requires hundreds of GPU hours leading to enormous amounts of carbon emission which has adverse environmental impacts [24].

There have been several attempts by researchers to reduce the reliance on large datasets. A naive approach to overcome this issue could be to randomly sample a subset from the original dataset and use it for training. However, such subsets need not necessarily reflect the diversity and information captured by original datasets. Another common approach has been that of Core-Subset or ‘Coreset’ selection [3, 6, 15, 39, 40, 47], which attempts to sample a small (*informative*) subset of the original data that can produce results comparable to the original dataset. However, finding an optimal solution to such a problem is NP-hard and often results in subpar performance. Further, it is shown that coreset methods scale poorly with the dimension of dataset leading to suboptimal subsets in higher dimensions [36].

To address these issues, [36] proposed ‘Bayesian Psuedo-Coreset’ (BPC), a new technique for generating synthetic images that can scale to high-dimensional datasets. The general idea of BPC is to use gradient based optimization to reduce the divergence between the parameter posterior of the original dataset and the parameter posterior associated with the synthetic dataset.

A parallel and closely related approach with same motivation is that of dataset condensation [7, 37, 45, 50, 52–54]. The goal of these methods is same as that of bayesian pseudo-coreset. However, these methods take a non-bayesian approach to generate the synthetic dataset by optimizing heuristic objectives based on features [45, 52], gradients [53], training trajectory [7], and performance matching [37, 54] between synthetic data samples and the original data points.

Recently, [25] tried to bridge the gap between bayesian pseudo-coreset (BPC) methods and dataset condensation methods by analyzing various divergence metrics. In particular, they showed that under certain assumptions, dataset condensation methods can be seen as special cases of BPC methods with different divergence metrics. However, on high dimensional datasets such as images, dataset condensation methods often outperform the performance of BPC methods.

We argue that this drop in performance is attributed to the stringent form of parameter posterior of original dataset used by previous methods. In this work, we relax this condition and propose a more flexible framework to work with such posteriors. In particular, we don't assume any form for parameter posterior associated with original dataset and use an energy-based distribution to model the posterior associated with synthetic data. Then, we derive contrastive divergence like loss function required to minimize the forward KL-Divergence between these posteriors. Our method allows flexibility to use various energy function without worrying about parameter posterior of original dataset. We experimentally observe that our method not only outperforms bayesian pseudo-coreset methods, but also gives performance comparable with that of dataset condensation methods. To the best of our knowledge, this is the first work that bridges the performance gap between BPC and dataset condensation methods. Our contributions can be summarized as follows :

- We propose a flexible framework for construction of bayesian pseudo-coreset where we don't assume any form for parameter posterior associated with original dataset and use a energy-based distribution to model the posterior associated with synthetic data.
- Our method allows one to use various energy functions to model the parameter posterior associated with synthetic data without having to worry about posterior associated with real data.
- We derive a contrastive-divergence like loss function to minimize the forward KL divergence between the posteriors; further, we also show a simple and efficient way to estimate this loss and learn the pseudo-coreset.
- We rigorously test our method against state-of-the-art BPC methods as well as dataset condensation methods. We observe that our method not only outperforms BPC methods but also gives performance comparable to that of dataset condensation, hence, bridging the performance gap between the two paradigms.

2. Related Work

2.1. Coreset

The idea of using less amount of data to achieve performance comparable to that obtained by using the entire dataset was first manifested by Coresets [3, 6, 15, 39, 40, 47]. The underlying idea of coreset methods is to select a subset of the training dataset that can achieve performance comparable to the original dataset. Herding based coreset methods [3, 6, 39, 47] select such samples by minimizing the distance between the feature centroid for the coreset and the feature centroid for the complete dataset. [47] proposed a greedy technique for constructing such a coreset by progressively and greedily adding data points that reduce the distance between these centroids. This strategy ensures that the most representative samples of the entire dataset are included in the subset, which is then used to train the model. However, herding based coreset often fails to sample a diverse group of data points, which impacts generalization capability of the model. In contrast to herding-based methods, K-center based coreset techniques [15, 40] pick the most diverse and representative samples by optimizing a minimax facility location-based submodular function [15]. Such method have also been explored in generative models to select the most representative sample during the learning process [43]. Contrary to K-center and herding based coreset selection methods, forgetting based coreset [44] removes the easily forgettable samples from the training dataset. This ensures that the coreset sampling process considers the uncertainty associated with the given model. Apart from the given methods, dataset subset selection has been explored in other fields like continual learning [5], active learning [27] and hyperparameter optimization [24].

2.2. Dataset Condensation

While coreset methods select a diverse and rich subset of data points from the training set, the basic heuristics used for subset selection often produce suboptimal results. To overcome this barrier [46] proposed Dataset Distillation to 'learn' a set of informative synthetic samples from a large dataset. Rather than selecting a subset of datapoints from the training set, these methods create an artificial dataset with a lower cardinality that, when trained independently, produces accuracy comparable to the original model.

In particular, the authors of [46] learn a model by using the synthetic set and test the model on original dataset. The synthetic set is optimized to improve the performance of the model on the original dataset. [26] further extended this idea by generating multiple synthetic dataset for training but with limited storage capacity. Inspired by these works, [53] proposed gradient matching where the authors proposed to learn the synthetic samples by aligning the gradients of models trained using original dataset and the syn-

thetic dataset. Despite the simplicity of gradient matching, it treats the gradients of each class independently, hence neglecting the class-discriminative features. To ensure that efficient gradients are calculated during the training process, some studies [22, 33, 49] have proposed different gradient comparison metrics that penalise the model for overfitting on the small dataset. Further, [50] proposed differentiable siamese augmentation to avoid overfitting and boost the performance of any dataset condensation method in general.

Further, methods like [9, 46] attempt to directly optimize the validation loss over samples of original dataset using the optimal parameters generated by the synthetic dataset. The validation loss is backpropagated through the unrolled gradient descent steps used for finding the optimal parameters. The overall idea is similar to that of meta-learning [16], where a bi-level optimization is performed to optimize (outer-loop) the meta-test loss in the original dataset using a model that has been meta-trained (inner-loop) on synthetic data. However, the computation graph for such methods increases with the number of steps in the inner-loop, which is computationally expensive and requires large GPU memory. To overcome this bottleneck, there have been methods that try to reduce the computational burden due to inner-loop. For eg. [37] proposes to approximate the inner-loop optimization by a convex optimization problem which can be solved using kernel ridge regression (KRR). [37] uses a neural tangent kernel (NTK) [21] to perform KRR. Further, to reduce the complexity involved in computing NTK, [35] uses a neural network gaussian process kernel instead. Further, [54] proposes to decompose the network optimized in the inner-loop into a feature-extractor and a linear classifier; they show that it is enough to update the linear classifier in the inner-loop while the feature extractor can be updated on synthetic set separately.

Contrary to bi-level optimization approaches that focus on short-horizon inner-loop trajectories, [7] proposes to focus on long-horizon trajectories, ensuring that the models learn comparable trajectories during optimization for both the synthetic set and the original dataset. To do this, the parameters of the model generated during training with synthetic data and with the original data are compared at different epochs. As a follow-up work, [34] showed that matching all the parameters has a negative impact on the performance of the model and the performance can be boosted by comparing a pruned set of parameters. Similarly, [12] proposed a regularizer to reduce the accumulated error in the long horizon trajectories. However, even though the trajectory based methods show high performance on several datasets, they suffer from same issues as that of meta-learning methods, i.e., the computational graph of such methods can be very large, leading to a high GPU memory requirement.

While the above mentioned methods resort to bi-level

optimization to learn the synthetic set, Distribution Matching methods [45, 51, 52] try to generate a condensed synthetic set with a similar feature distribution as the original dataset, hence, completely avoiding the bi-level optimization. For eg. [52] proposed to use maximal mean discrepancy (MMD) to match the distribution of the synthetic dataset with the original dataset using the classifier layer without the last linear layer. [45] further proposed CAFE to match feature statistics of different layers and used a discriminator to maximise the probability for a given class.

2.3. Bayesian Psuedo-Coreset

Recently, there has been a surge in methods that try to re-interpret the existing deep learning methods from a bayesian perspective. For eg. [23] showed that most of the machine learning algorithms and practices are special instances of a generic algorithm, namely, the Bayesian Learning Rule. Following this line of thought, [36] proposed a bayesian perspective to dataset condensation. Particularly, they formulate dataset condensation as a divergence minimization problem between the parameter posteriors associated with synthetic set and the original dataset. The synthetic set obtained using such methods is termed as ‘Bayesian Pseudo-Coreset’ (BPC). Compared to corsets, these methods scale more efficiently with data dimensions and achieve a better posterior approximation. Furthermore, a bayesian formulation of the given problem further enhances the understanding of the given field.

The main idea proposed in BPC-methods is to minimize the divergence between the posterior associated with psuedocoreset and the original training dataset. [36] formalized the given problem by minimising the reverse-KL divergence between posterior of real data with the posterior of synthetic data. On similar lines, [25] demonstrated that other divergence metric, such as wasserstein distance and forward-KL divergence, can also be used to generate comparable accuracy. Further, [25] showed that under certain assumptions, dataset condensation methods can be looked into as special instances of BPC-methods. For eg. MTT [7] can be shown as BPC-method with wasserstein distance as the divergence metric. Similarly, gradient matching [53] can be shown as a BPC-method under reverse-KL divergence as the divergence metric. Further, [25] proposes to use forward KL divergence as the divergence metric as it encourages the model to cover the entire target distribution. However, despite the theoretical support for these methods, there are lot of stringent assumptions involved in formulation of posteriors associated with synthetic set and original dataset. Moreover, there is still a significant performance gap between BPC methods and dataset condensation methods, which we have attempted to bridge through our work.

2.4. Energy Based Models

Energy Based Models or EBMs are a class of density estimation models that assume the required density to have the form of an energy-based distribution. In particular, the desired density ($p(x)$) is approximated by a parametric density of the form $p_\theta(x) = \exp(-E_\theta(x))/Z_\theta$ where $E_\theta(\cdot)$ is the negative log of un-normalized density also called the energy function and $Z_\theta = \int_x \exp(-E_\theta(x))dx$ is the normalizing constant also known as the partition function. Generally, the goal of EBMs is to learn the parameters θ of the energy function that minimizes the KL divergence between the desired density and $p_\theta(x)$. There have been several lines of work that try to train the EBMs efficiently [2, 13, 14, 17] however, the most simple and commonly used approach is the one proposed in [14]. Particularly, the contrastive-divergence loss used to learn the parameters of the energy function as shown in [20] is given by:

$$\mathcal{L} = \mathbb{E}_{x^+ \sim p(x)}[E_\theta(x^+)] - \mathbb{E}_{x^- \sim p_\theta(x)}[E_\theta(x^-)] \quad (1)$$

The above loss function ensures that the model learns to assign low energy to the samples associated with the real data points and high energy to samples obtained from the parametric density. The first expectation in above expression is approximated using the samples present in the dataset. However, we cannot directly get samples from $p_\theta(\cdot)$ to approximate the second expression, as the partition function is intractable and sampling would be very inefficient. To overcome this bottleneck, we resort to gradient-based markov-chain monte-carlo (MCMC) methods such as langevin dynamics to sample from $p_\theta(\cdot)$.

In the following work, we approximate the parameter posterior associated with synthetic set by an energy-based distribution, however, in our case the goal is not to learn the parameters of the energy function but to learn the synthetic set itself. Hence, we fix the energy function and derive a loss function (similar to contrastive-divergence) to learn the synthetic samples instead. The rest of the paper is organized as follows: In Section 3.1, we setup the notations and formalize our problem statement, in Section 3.2 we derive the loss function used to construct the pseudo-coreset and describe the proposed method. In Section 4, we provide the implementation details of the proposed method. Lastly, in Section 5, we present our experimental findings and compare it with previous baselines.

3. Proposed Method

3.1. Overview

Consider the training set $\mathcal{D} = \{(\mathbf{x}_i, y_i)\}_{i=1}^{|\mathcal{D}|}$ where, the cardinality of the dataset is $|\mathcal{D}|$. The goal of bayesian pseudo-coreset is to construct a sythetic dataset $\tilde{\mathcal{D}} = \{\tilde{\mathbf{x}}_i, \tilde{y}_i\}_{i=1}^{|\tilde{\mathcal{D}}|}$ such that $\{y_i\}$ and $\{\tilde{y}_i\}$ share the same label

space and $|\tilde{\mathcal{D}}| \ll |\mathcal{D}|$; further, $\tilde{\mathcal{D}}$ should provide classification performance that is comparable to that of original training set \mathcal{D} . For this, consider the space of parameters of a discriminative / classification model (Θ). Now, let $\mathbf{p}(\theta|\mathcal{D})$ and $\mathbf{q}(\theta|\tilde{\mathcal{D}})$ be the density of optimal parameters induced due to the original training set (\mathcal{D}) and the synthetic set ($\tilde{\mathcal{D}}$) respectively. In particular, let \mathcal{F} be the space of all classification loss functions. Now, let

$$\mathcal{M}_\ell = \left\{ \theta \in \Theta : \arg \min_{\theta} \frac{1}{|\mathcal{D}|} \sum_{i=1}^{|\mathcal{D}|} \ell(y_i, f_\theta(\mathbf{x}_i)) \right\} \quad (2)$$

be the set of all parameters that minimize the empirical risk w.r.t some loss function $\ell(\cdot) \in \mathcal{F}$ and classifier $f_\theta(\cdot)$ manifested by θ . Then, $\mathbf{p}(\theta|\mathcal{D})$ can be seen as the distribution induced on union of all such sets, i.e.,

$$\bigcup_{\ell \in \mathcal{F}} \mathcal{M}_\ell \sim \mathbf{p}(\theta|\mathcal{D}) \quad (3)$$

Similarly, we can define $\tilde{\mathcal{M}}_\ell$ to be the set of parameters that minimize the empirical risk for synthetic set $\tilde{\mathcal{D}}$, and $\mathbf{q}(\theta|\tilde{\mathcal{D}})$ can be seen as the distribution induced on union of all such sets:

$$\bigcup_{\ell \in \mathcal{F}} \tilde{\mathcal{M}}_\ell \sim \mathbf{q}(\theta|\tilde{\mathcal{D}}) \quad (4)$$

Note that we don't know the closed-form expressions for the above densities. Previous methods [25, 36] assume some form for $\mathbf{p}(\theta|\mathcal{D})$ and $\mathbf{q}(\theta|\tilde{\mathcal{D}})$, however, this is not desirable as these densities can be very complex and assuming distributional form for these densities would reduce the flexibility for constructing the synthetic set of pseudo-coreset. Hence, in this work, we don't assume any form for $\mathbf{p}(\theta|\mathcal{D})$, however, we assume an energy-based distribution for $\mathbf{q}(\theta|\tilde{\mathcal{D}})$, i.e., $\mathbf{q}(\theta|\tilde{\mathcal{D}}) = \exp(-E(\theta, \tilde{\mathcal{D}}))/Z(\tilde{\mathcal{D}})$. Note that, here the energy function $E(\theta, \tilde{\mathcal{D}})$ is fixed and is not learnable, however, $\tilde{\mathcal{D}}$ is a learnable quantity. First, we will show the loss for any generic energy function, later we analyze and discuss the effect of different choices for energy functions.

While dataset condensation methods (cf. Sec. 2.2) resort to heuristics to construct the synthetic set; bayesian pseudo-coresets explicitly minimize a divergence metric between $\mathbf{p}(\theta|\mathcal{D})$ and $\mathbf{q}(\theta|\tilde{\mathcal{D}})$. In our method, we propose to construct the pseudo-coresets by solving the following optimization problem:

$$\tilde{\mathcal{D}}^* = \arg \min_{\tilde{\mathcal{D}}} D_{KL}(\mathbf{p}(\theta|\mathcal{D}) || \mathbf{q}(\theta|\tilde{\mathcal{D}})) \quad (5)$$

where, D_{KL} is the forward-KL divergence, $\mathbf{p}(\theta|\mathcal{D})$ is parameter posterior associated with original training set and $\mathbf{q}(\theta|\tilde{\mathcal{D}})$ is the parameter posterior associated with the pseudo-coreset which has a form of generic energy-based distribution.

3.2. Problem Formulation

As mentioned in the previous section, our aim is to minimize the forward-KL divergence between $\mathbf{p}(\theta|\mathcal{D})$ and $\mathbf{q}(\theta|\tilde{\mathcal{D}})$ w.r.t $\tilde{\mathcal{D}}$, where $\mathbf{p}(\theta|\mathcal{D})$ can have any distributional form and $\mathbf{q}(\theta|\tilde{\mathcal{D}}) = \exp(-E(\theta, \tilde{\mathcal{D}}))/Z(\tilde{\mathcal{D}})$. To obtain the synthetic set that minimizes the above divergence metric, we take the gradient of above expression w.r.t $\tilde{\mathcal{D}}$:

$$\nabla_{\tilde{\mathcal{D}}} D(\mathbf{p}(\theta|\mathcal{D})||\mathbf{q}(\theta|\tilde{\mathcal{D}})) = \nabla_{\tilde{\mathcal{D}}} \mathbb{E}_{\mathbf{p}(\theta|\mathcal{D})} \left[\log \left(\frac{\mathbf{p}(\theta|\mathcal{D})}{\mathbf{q}(\theta|\tilde{\mathcal{D}})} \right) \right] \quad (6)$$

$$= -\nabla_{\tilde{\mathcal{D}}} \mathbb{E}_{\mathbf{p}(\theta|\mathcal{D})} \left[\log \left(\frac{\exp(-E(\theta, \tilde{\mathcal{D}}))}{Z(\tilde{\mathcal{D}})} \right) \right] \quad (7)$$

$$= -\nabla_{\tilde{\mathcal{D}}} \left[\int (-E(\theta, \tilde{\mathcal{D}}) - \log(Z(\tilde{\mathcal{D}}))) \mathbf{p}(\theta|\mathcal{D}) d\theta \right] \quad (8)$$

$$= \int \nabla_{\tilde{\mathcal{D}}} E(\theta, \tilde{\mathcal{D}}) \mathbf{p}(\theta|\mathcal{D}) d\theta + \int \nabla_{\tilde{\mathcal{D}}} \log(Z(\tilde{\mathcal{D}})) \mathbf{p}(\theta|\mathcal{D}) d\theta \quad (9)$$

$$= \mathbb{E}_{\mathbf{p}(\theta|\mathcal{D})} [\nabla_{\tilde{\mathcal{D}}} E(\theta, \tilde{\mathcal{D}})] - \mathbb{E}_{\mathbf{q}(\theta|\tilde{\mathcal{D}})} [\nabla_{\tilde{\mathcal{D}}} E(\theta, \tilde{\mathcal{D}})] \quad (10)$$

Taking the monte-carlo approximation of the above loss function, the final loss function comes out be:

$$\mathcal{L} = \mathbb{E}_{\theta^+ \sim \mathbf{p}(\theta|\mathcal{D})} [E(\theta^+, \tilde{\mathcal{D}})] - \mathbb{E}_{\theta^- \sim \mathbf{q}(\theta|\tilde{\mathcal{D}})} [E(\theta^-, \tilde{\mathcal{D}})] \quad (11)$$

As it can be seen, the above loss function looks similar to the contrastive-divergence loss in Eq. (1). However, instead of learning the parameters of an energy-based model [14], we use it to learn the pseudo-coreset.

Now, to estimate the expectation terms in Eq. (11) we need to sample the parameters (θ) from the posteriors $\mathbf{p}(\theta|\mathcal{D})$ and $\mathbf{q}(\theta|\tilde{\mathcal{D}})$. As mentioned earlier, we don't assume any distributional form for $\mathbf{p}(\theta|\mathcal{D})$, hence we use the parameters obtained by training a model on the original training set (\mathcal{D}) to approximate the first expectation. Specifically, we train a classification model with parameters θ on the training set \mathcal{D} with some classification loss $\ell_{\mathcal{D}} \in \mathcal{F}$. Next, to evaluate the second expectation, we resort to langevin dynamics to sample θ from $\mathbf{q}(\theta|\tilde{\mathcal{D}})$. Langevin dynamics is an iterative gradient-based MCMC sampling methods given by the following update rule:

$$\theta^{(t+1)} = \theta^{(t)} - \frac{\alpha}{2} \nabla_{\theta^{(t)}} E(\theta, \tilde{\mathcal{D}}) + \sqrt{\alpha} \eta, \quad \eta \sim \mathcal{N}(0, I) \quad (12)$$

From an implementation perspective, the above is similar to running a noisy gradient descent on parameters to minimize the chosen energy function.

3.3. Choice of Energy Function

Till now, we have worked with a generic energy function $E(\cdot)$. In this section, we motivate the choices for energy

function. It can be seen from Eq. (12) that the sampled θ will be such that it minimizes the chosen energy function, $E(\cdot)$. However, from Eq. (4) we also know that the set of desired $\theta \in \Theta$ are such that they minimize a class of loss functions. Hence, a logical choice for the energy function is a classification loss function itself! In other words we can choose the energy function $E(\cdot)$ to be a classification loss $\ell_{\tilde{\mathcal{D}}} \in \mathcal{F}$ so that, sampling from $\mathbf{q}(\theta|\tilde{\mathcal{D}})$ is equivalent to training a network with parameters θ on $\tilde{\mathcal{D}}$ with loss function $\ell_{\tilde{\mathcal{D}}}$. Further, with this choice of energy function, we can see that Eq. (11) is nothing but difference between average loss (w.r.t $\ell_{\tilde{\mathcal{D}}}$) incurred on parameters obtained from training on original training set and parameters obtained from training on the synthetic set.

To this end, we propose to use the categorical cross-entropy as the energy function, i.e.,

$$E(\theta, \tilde{\mathcal{D}}) = -\frac{1}{|\tilde{\mathcal{D}}|} \sum_{i=1}^{|\tilde{\mathcal{D}}|} \sum_{j=1}^C \tilde{y}_i^{(j)} \log f_{\theta}(\tilde{x}_i)^{(j)} \quad (13)$$

where, $f_{\theta}(\cdot)$ is the classifier manifested by parameters θ and $\tilde{y}_i^{(j)}$ is the indicator for the j^{th} true class. One can also choose other classification losses such as Focal loss and Multi-Margin Loss. We explore the effect of such choices in Section 5.5.

4. Implementation

The implementation of the proposed method is inspired from MTT [7]. Our entire training process can be divided into two parts. Firstly, we generate a set of parameters associated with the posterior defined on the real dataset, ($\mathbf{p}(\theta|\mathcal{D})$). To do this, we train multiple instances of networks with different initialization to minimize the empirical risk w.r.t to loss, $\ell_{\mathcal{D}}$ on the original dataset (\mathcal{D}). We save a copy of the optimal parameters after each epoch for a given initialization. A sequence of such parameters is referred to as a trajectory (similar to MTT [7]) in our discussion. We store multiple such trajectories in a buffer to estimate the first expectation in Eq. (11).

Secondly, we sample parameters from the posterior associated with the synthetic set i.e., $\mathbf{q}(\theta|\tilde{\mathcal{D}})$. For this, we first sample a trajectory from the buffer obtained above, $\tau_i \sim \tau$. Next, we choose an instantiation of parameters at a randomly chosen epoch associated with τ_i , ($\theta_k^+ \sim \tau_i$). Further, we use the T -step horizon from θ_k^+ as a proxy for θ^+ in Eq. (11) i.e., $\theta^+ = \theta_{k+T}^+$. To sample θ^- , we use L -step langevin dynamics updates as shown in Eq. (12), with $\theta^{(0)} = \theta_k^+$. After this, we pass the synthetic set ($\tilde{\mathcal{D}}$) through the networks manifested by θ^+ and θ^- to calculate the respective energies, $E(\theta^+, \tilde{\mathcal{D}})$ and $E(\theta^-, \tilde{\mathcal{D}})$ to further calculate the contrastive-divergence (Eq. (11)). The gradients of the contrastive-divergence are then backpropagated to up-

date the synthetic set \tilde{D} . We plan to make our codebase public post acceptance for better reproducibility.

5. Experiments

In this section, we present the performance and experimental findings pertaining to the proposed method. We evaluate our method both quantitatively and qualitatively on several BPC-benchmark datasets with different compression ratios, i.e., the number of images generated per class (ipc). In particular, we perform our experiments on six different datasets, namely, CIFAR10 [28], SVHN [41], MNIST [32] and FashionMNIST [48]. We also test our method on some difficult datasets such as CIFAR100 [28] and Tiny Imagenet [31]. We set ipc=1/10/50 for each of the above datasets. Further, we use a standard ConvNet architecture for all the experiments unless mentioned otherwise.

Next, since our method relies on posteriors of parameters and the parameters are associated with a particular network architecture, the cross-architecture analysis becomes essential. We show cross-architecture performance for our method and compare it with other state-of-the-art BPC methods. Further, we explore different choices for the energy function used in our method and show the effect of such choices. We also investigate how the training time scales under each epoch while there is an increase in images per class for the CIFAR10 dataset. We also examine the consumption of GPU memory on individual methods when the synthetic set expands.

5.1. Baselines

Our proposed method primarily falls under the category of Bayesian Pseudo-Coreset due to the formulation shown in Section 3. Hence, we consider the previous BPC methods for comparison. In particular, we include the BPC formulation using reverse-KL Divergence (BPC-rKL) [36], forward-KL Divergence (BPC-fKL) [25] and Wasserstein metric (BPC-W) [25] for comparison. Additionally, we also show that our method gives best if not second best performance compared to other baselines. Hence, we include eight dataset-condensation baselines for comparison. Particularly, we include Dataset Distillation (DD) [46], Flexible Dataset Distillation (LD) [4], Gradient Matching (DC) [53], Differentiable Siamese Augmentation (DSA) [50], Distribution Matching (DM) [52], Neural Ridge Regression (KIP) [37], Condensed data to align features (CAFE) [45] and Matching Training Trajectories (MTT) [7] for comparison. In addition, for the sake of completeness, we include the major Coreset selection baselines such as Herding [8], k-Center and Forgetting [44] for comparison.

5.2. Performance on Low-Resolution Datasets

Firstly, we present the results on low-resolution datasets like MNIST, FashionMNIST (FMNIST), SVHN, and CIFAR10. Our findings are listed in Table 1. In particular, we observe that the proposed method significantly outperforms all the BPC methods by large margins, for e.g. we observe a gain of 11.3%, 6.54% and 21.01% on CIFAR10 with an ipc of 1, 10 and 50 respectively compared to the best performing BPC baselines. Similarly, on SVHN we observe gain of 18.72%, 6.83% and 8.92% respectively compared to the BPC counterparts. A similar trend can be seen for MNIST and FMNIST as well. We attribute this boost in performance to the flexible formulation of the proposed method.

Further, we observe that our method not only outperforms BPC methods but also outperforms SoTA dataset condensation methods in most of the cases. We find that our performance is better than almost all the dataset condensation baselines whereas MTT stands out to be a close second in most of the cases. For e.g. we see a gain of 0.79% and 0.67% on CIFAR10 with ipc of 1 and 50 respectively when compared to MTT, however, there is a loss of about 7.88% with ipc of 10. Further, there is a gain of 9.19%, 3.93% and 4.68% on SVHN dataset with ipc of 1, 10 and 50 respectively when compared to the corresponding best performance of dataset condensation methods. We can observe similar trends for MNIST as well as FMNIST datasets. This shows that our method although falling under the category of bayesian pseudo-coreset, achieves a performance which is comparable to that of heuristic dataset condensation.

We present the qualitative visualizations for MNIST, FMNIST, SVHN, and CIFAR10 datasets with 1 and 10 images per class. It can be seen that, for one image per class, our method can do an excellent job condensing the whole dataset and achieving formidable results. The constructed pseudo-coreset is identifiable but inherits some artifacts due to the constraints on the dataset size. As the number of images per class increases, the model can induce more variations across all the classes and thus produce a diverse pseudo-coreset. This can be observed in Figure 2 where we show the synthetic set generated with 10 images per class.

5.3. Performance on larger datasets

Next, we show the efficacy of proposed method on larger datasets with relatively high-resolution. For this, we choose the standard benchmark datasets of CIFAR100 and Tiny ImageNet. CIFAR100 contains images of size 32×32 under 100 diverse classes such as aquatic mammals, fish, flowers, food containers, household furniture, insects, etc. Further, Tiny ImageNet is a subset of the famous ImageNet dataset with each image of size 64×64 under 200 classes. The large number of classes for these datasets make the condensation

	MNIST			FMNIST			SVHN			CIFAR10		
Img/Cls	1	10	50	1	10	50	1	10	50	1	10	50
Ratio%	0.017	0.17	0.83	0.017	0.17	0.83	0.014	0.14	0.7	0.02	0.2	1
DD [46]	-	79.71 \pm 8.3	-	-	-	-	-	-	-	-	39.14 \pm 2.3	-
LD [4]	60.6 \pm 2.86	87.05 \pm 0.5	93.3 \pm 0.3	-	-	-	-	-	-	25.38 \pm 0.2	37.5 \pm 0.6	41.7 \pm 0.5
Herding [6, 47]	89.2 \pm 1.6	93.7 \pm 0.3	94.8 \pm 0.2	67.0 \pm 1.9	71.1 \pm 0.7	71.9 \pm 0.8	20.9 \pm 1.3	50.5 \pm 3.3	72.6 \pm 0.8	21.5 \pm 1.2	31.6 \pm 0.7	23.3 \pm 1.0
K-Center [15, 40]	89.3 \pm 1.5	84.4 \pm 1.7	97.4 \pm 0.3	66.9 \pm 1.8	54.7 \pm 1.5	68.3 \pm 0.8	21.0 \pm 1.5	14.0 \pm 1.3	20.1 \pm 1.4	21.5 \pm 1.3	14.7 \pm 0.9	27.0 \pm 1.4
Forgetting [44]	35.5 \pm 5.6	68.1 \pm 3.3	88.2 \pm 1.2	42.0 \pm 5.5	53.9 \pm 2.0	55.0 \pm 1.1	12.1 \pm 1.7	16.8 \pm 1.2	27.2 \pm 1.5	13.5 \pm 1.2	23.3 \pm 1.0	23.3 \pm 1.1
Random	64.9 \pm 3.5	95.1 \pm 0.9	97.9 \pm 0.2	51.4 \pm 3.8	73.8 \pm 0.7	82.5 \pm 0.7	14.6 \pm 1.6	35.1 \pm 4.1	70.9 \pm 0.9	14.4 \pm 2.0	26.0 \pm 1.2	43.4 \pm 1.0
BPC-rKL(sghmc) [25, 36]	74.8 \pm 1.17	95.27 \pm 0.17	94.18 \pm 0.26	70.53 \pm 1.09	78.81 \pm 0.17	76.97 \pm 0.59	18.34 \pm 1.79	60.68 \pm 5.07	78.27 \pm 0.62	21.62 \pm 0.83	37.89 \pm 1.54	37.54 \pm 1.32
BPC-W(sghmc) [25]	83.59 \pm 1.49	91.72 \pm 0.55	93.72 \pm 0.55	72.39 \pm 0.87	83.69 \pm 0.51	74.41 \pm 0.48	33.52 \pm 1.15	74.75 \pm 1.27	79.49 \pm 0.54	29.34 \pm 1.21	48.9 \pm 1.72	46.17 \pm 0.67
BPC-fKL(sghmc) [25]	82.98 \pm 2.2	92.05 \pm 0.42	40.63 \pm 1.8	72.51 \pm 2.53	83.29 \pm 0.55	74.82 \pm 0.52	21.48 \pm 6.58	75.49 \pm 0.84	77.08 \pm 1.8	29.3 \pm 1.1	49.85 \pm 1.37	42.30 \pm 2.87
BPC-fKL(hmc) [25]	90.46 \pm 1.5	89.8 \pm 0.82	95.58 \pm 1.63	78.24 \pm 1.02	82.06 \pm 0.44	82.40 \pm 0.35	48.02 \pm 5.62	65.64 \pm 2.92	79.6 \pm 0.53	35.57 \pm 0.95	43.07 \pm 1.06	50.92 \pm 1.49
DC [53]	92.01 \pm 0.25	97.58 \pm 0.1	98.81 \pm 0.03	70.83 \pm 0.01	81.93 \pm 0.07	83.26 \pm 0.17	30.49 \pm 0.57	75.1 \pm 0.4	81.7 \pm 0.14	28.10 \pm 0.56	44.14 \pm 0.6	53.73 \pm 0.44
DSA [50]	87.6 \pm 0.07	97.39 \pm 0.06	98.87 \pm 0.04	70.45 \pm 0.57	84.7 \pm 0.11	88.55 \pm 0.56	31.18 \pm 0.43	78.39 \pm 0.3	82.5 \pm 0.34	29 \pm 0.64	51.85 \pm 0.43	60.77 \pm 0.45
DM [52]	88.89 \pm 0.57	96.58 \pm 0.11	98.22 \pm 0.05	71.92 \pm 0.7	83.25 \pm 0.09	87.65 \pm 0.03	19.25 \pm 1.39	71.42 \pm 1.01	82.41 \pm 0.52	26.40 \pm 0.42	48.66 \pm 0.03	62.7 \pm 0.07
KIP [37]	85.46 \pm 0.04	97.15 \pm 0.11	98.36 \pm 0.08	-	-	-	-	-	-	40.5 \pm 0.4	53.1 \pm 0.5	58.6 \pm 0.4
CAFE [45]	93.1 \pm 0.3	97.2 \pm 0.2	98.6 \pm 0.2	77.1 \pm 0.9	83.0 \pm 0.4	84.8 \pm 0.4	42.6 \pm 3.3	75.9 \pm 0.6	81.3 \pm 0.3	30.3 \pm 1.1	46.3 \pm 0.6	55.5 \pm 0.6
CAFE+DSA [45]	90.8 \pm 0.5	97.5 \pm 0.1	98.9 \pm 0.2	73.7 \pm 0.7	83.0 \pm 0.3	88.2 \pm 0.3	42.9 \pm 3.0	77.9 \pm 0.6	82.3 \pm 0.4	31.6 \pm 0.8	50.9 \pm 0.5	63.3 \pm 0.4
MTT [7]	89.85 \pm 0.01	97.7 \pm 0.02	98.6 \pm 0.006	77.14 \pm 0.007	88.768 \pm 0.00158	89.332 \pm 0.151	57.55 \pm 0.02	72.56 \pm 0.005	83.731 \pm 0.334	46.08 \pm 0.8	64.27 \pm 0.8	71.26 \pm 0.5
Ours	93.42 \pm 0.09	97.71 \pm 0.24	98.91 \pm 0.22	77.29 \pm 0.5	88.40 \pm 0.21	89.47 \pm 0.06	66.74 \pm 0.09	82.32 \pm 0.56	88.41 \pm 0.12	46.87 \pm 0.2	56.39 \pm 0.7	71.93 \pm 0.17
Whole Dataset	-	99.6 \pm 0.0	-	-	93.5 \pm 0.1	-	-	95.4 \pm 0.1	-	-	84.8 \pm 0.1	-

Table 1. Performance comparison of Coreset, BPC and Dataset Condensation methods for MNIST, FashionMNIST, SVHN and CIFAR10 datasets. The results are noted in form of (mean \pm std. dev) where we have obtained test accuracy over five independent runs on the pseudo-coreset. The best performer for each set of methods is denoted by an underline ($\underline{x} \pm s$). The best performer across all methods is denoted in bold ($\mathbf{x} \pm s$). For ease of comparison, we color the best performer with green color and the second best performer with orange color.



Figure 1. Visualizations of pseudo-coreset with one image per class for MNIST, FMNIST, SVHN and CIFAR10.

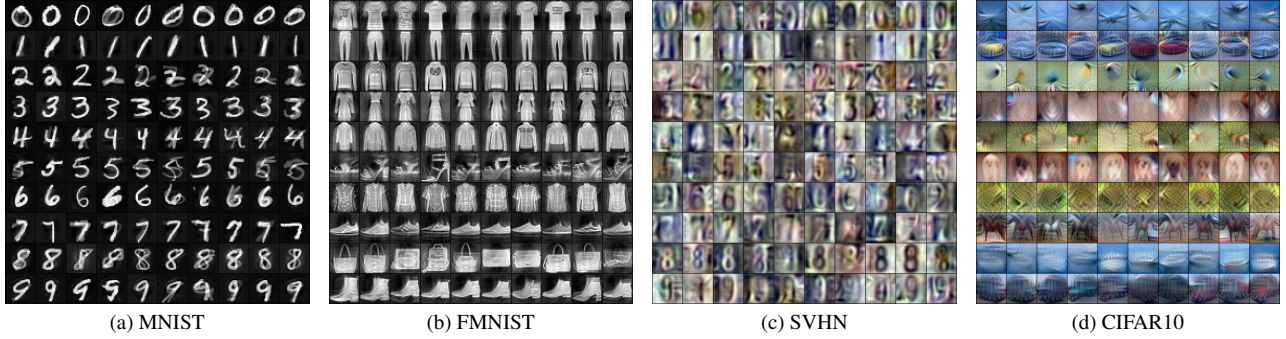


Figure 2. Visualizations of pseudo-coreset with ten image per class for MNIST, FMNIST, SVHN and CIFAR10.

and creation of pseudo-coreset difficult.

Our findings are presented in Table 2. Our observation is in line with that on low-resolution dataset discussed in previous section. In particular, our method outperforms previous SoTA BPC methods by large margin. For e.g. we see an increment of 11.78% on CIFAR100 with an ipc of 1. Further, our method achieves performance comparable to that of dataset condensation methods. It can be seen from Table 2 that our method outperforms MTT on CIFAR100 as well as Tiny ImageNet with an ipc of 1. However, MTT gives a gain of 8.54% compared to our method on CIFAR100 with ipc 10, which ranks us the third best amongst the baselines. Further, on Tiny ImageNet with ipc of 10, MTT gives a boost of 2.29% relative to our performance, ranking us the second best in this setting.

5.4. Cross Architecture Analysis

As discussed in previous sections, BPC methods rely on divergence minimization between posteriors associated with original training set and synthetic set. Hence, a natural concern that arises is that of generalization of such synthetic set across different network architecture. While this aspect of synthetic set is explored in dataset condensation literature, BPC literature have not addressed this concern. For this reason, we show the cross-architecture generalization of synthetic sets generated using BPC methods. For this, we construct the pseudo-coreset for CIFAR10 (ipc=10) by using a ConvNet architecture mentioned in previous section, and train different networks like ResNet [19], VGG [42] and AlexNet [30] on the pseudo-coreset to test the generalization of the network. Our findings are listed in Table 3. It can be seen that previous BPC methods lack to generalize across

	CIFAR100		TinyImagenet	
	1 0.2	10 2	1 0.2	10 2
LD [4]	<u>11.5 ± 0.4</u>	-	-	-
Random	4.2 ± 0.3	14.6 ± 0.5	1.4 ± 0.1	5.0 ± 0.2
Forgetting [44]	4.5 ± 0.2	15.1 ± 0.3	1.6 ± 0.1	5.1 ± 0.2
K-Center [15, 40]	8.3 ± 0.3	7.1 ± 0.2	<u>3.03 ± 0.0</u>	<u>11.38 ± 0.0</u>
Herdin [6, 47]	8.4 ± 0.3	17.3 ± 0.3	2.8 ± 0.2	6.3 ± 0.2
BPC-rKL(sghmc) [25, 36]	3.56 ± 0.04	-	-	-
BPC-fKL(hmc) [25]	7.57 ± 0.54	-	-	-
BPC-fKL(sghmc) [25]	12.07 ± 0.16	-	-	-
BPC-W(sghmc) [25]	12.19 ± 0.22	-	-	-
DC [53]	12.65 ± 0.32	25.28 ± 0.29	5.27 ± 0.0	12.83 ± 0.0
DSA [50]	13.88 ± 0.29	32.34 ± 0.4	5.67 ± 0.0	16.43 ± 0.0
DM [52]	11.35 ± 0.18	29.38 ± 0.26	3.82 ± 0.0	13.51 ± 0.0
KIP [37]	12.04 ± 0.0	29.04 ± 0.0	-	-
CAFE [45]	12.9 ± 0.3	27.8 ± 0.3	-	-
CAFE+DSA [45]	14.0 ± 0.3	31.5 ± 0.2	-	-
MTT [7]	<u>23.62 ± 0.63</u>	<u>36.96 ± 0.155</u>	<u>8.27 ± 0.0</u>	<u>20.11 ± 0.00</u>
Ours	<u>23.97 ± 0.11</u>	28.42 ± 0.24	<u>8.39 ± 0.07</u>	17.82 ± 0.39
Whole Dataset	56.2 ± 0.3		39.83 ± 0.0	

Table 2. CIFAR100 and TinyImagenet results for 1 and 10 ipc on all the above methods. The best performer for each set of methods is denoted by an underline ($\underline{x \pm s}$). The best performer across all methods is denoted in bold ($\mathbf{x \pm s}$). For ease of comparison, we color the best performer with green color and the second best performer with orange color.

network architecture whereas our method is able to generalize well on other architectures as well. For instance, the performance of BPC-fKL and BPC-rKL drop by 34.19% and 24.42% respectively on ResNet resulting in random predictions with an accuracy of almost 10%, whereas our method observes a drop of only 14.74% while performing with an accuracy of 41.65%. The same pattern can be seen with other architectures, demonstrating that our approach is generalizable even when other BPC methods fail.

	ConvNet	ResNet	VGG	AlexNet
Ours	56.39 ± 0.7	41.65 ± 1.03	47.51 ± 0.89	30.58 ± 1.43
BPC-fKL	44.34 ± 1.11	10.15 ± 0.21	10.43 ± 0.33	10.0 ± 0.0
BPC-rKL	34.48 ± 0.48	10.06 ± 0.08	10.26 ± 0.35	10.0 ± 0.0

Table 3. Comparison of BPC methods on cross-architecture generalization. For this, we construct the pseudo-coreset for CIFAR10 by using ConvNet architecture, and test it on other architectures like ResNet [19], VGG [42] and AlexNet [30]. The best performer for each architecture is denoted in bold symbols.

5.5. Effect of choice of Energy function

As discussed in previous sections, our method requires creation of training trajectories from original dataset to sample from posterior associated with original dataset. This requires training of network parameters using a certain loss function, call it $\ell_{\mathcal{D}}(\cdot)$. Next, we use langevin dynamics to sample from posterior associated with synthetic set. As discussed in Section 3.3, this can be seen as learning of network parameters via noisy gradient descent on energy function. And as noted, it is logical to choose any loss function, call it $\ell_{\tilde{\mathcal{D}}}(\cdot)$, as the energy function. Hence, a natural question to follow is how does the choice of $\ell_{\mathcal{D}}$ and

$\ell_{\tilde{\mathcal{D}}}$ affect the performance of pseudo-coreset. For this, we do a ‘cross-loss’ analysis for our method, where we observe the effect of using different choices of $\ell_{\mathcal{D}}$ and $\ell_{\tilde{\mathcal{D}}}$. For this analysis, we use three candidate classification loss functions: Cross-entropy loss, Focal loss and Multi-margin classification loss. Our observations for CIFAR10 (ipc=10) are listed in Table 4. We observe that our method performs best for a certain loss function when $\ell_{\mathcal{D}} = \ell_{\tilde{\mathcal{D}}}$. This can be attributed to the fact that the posterior estimates are closer when same loss function is used to obtain the trained parameters. This can also be seen from the observation that when different losses are used i.e., when $\ell_{\mathcal{D}} \neq \ell_{\tilde{\mathcal{D}}}$, there is a drop in performance of pseudo-coresets. Further, we observe that amongst all the choices, cross-entropy loss provides the best result.

$\ell_{\mathcal{D}}(\cdot) \backslash \ell_{\tilde{\mathcal{D}}}(\cdot)$		Cross Entropy	Focal	Margin
Cross Entropy		56.39 ± 0.7	55.05 ± 0.28	45.68 ± 0.72
Focal		37.79 ± 0.12	54.24 ± 0.34	43.62 ± 0.11
Margin		52.09 ± 0.86	52.44 ± 0.82	53.91 ± 0.76

Table 4. Effect of choosing different training loss and energy function for construction of pseudo-coreset.

6. Conclusion

Dataset condensation and BPC methods address the issue of over reliance on large training datasets by generating a small synthetic set with comparable performance as the original training dataset. These methods not only reduces the training costs for downstream tasks, but also result in lower carbon emissions. There is, however, a significant performance gap between the BPC and dataset condensation techniques. This gap in performance for BPC methods can be attributed to the various assumptions made about the form of the posterior distribution. In our work, we address this issue by using an energy-based distribution to model the posterior associated with the synthetic set without making any assumption about the form of posterior for real dataset. We also derive a contrastive divergence-based loss to minimize the KL divergence between the posteriors associated with real and synthetic datasets. Our formulation not only outperforms other BPC methods but also bridges the performance gap between BPC and dataset condensation methods. A better understanding of theoretically grounded works such as BPC can not only improve the performance of standard classification tasks but also pave the way to extend these methods to other resource-intensive tasks. In the future, we intend to investigate BPC and dataset condensation techniques for large generative models.

References

- [1] Dario Amodei, Sundaram Ananthanarayanan, Rishita Anubhai, Jingliang Bai, Eric Battenberg, Carl Case, Jared Casper, Bryan Catanzaro, Qiang Cheng, Guoliang Chen, et al. Deep speech 2: End-to-end speech recognition in english and mandarin. In *International conference on machine learning*, pages 173–182. PMLR, 2016. 1
- [2] Michael Arbel, Liang Zhou, and Arthur Gretton. Generalized energy based models. In *International Conference on Learning Representations*, 2021. 4
- [3] Eden Belouadah and Adrian Popescu. Scail: Classifier weights scaling for class incremental learning. In *Proceedings of the IEEE/CVF winter conference on applications of computer vision*, pages 1266–1275, 2020. 1, 2
- [4] Ondrej Bohdal, Yongxin Yang, and Timothy Hospedales. Flexible dataset distillation: Learn labels instead of images. *arXiv preprint arXiv:2006.08572*, 2020. 6, 7, 8
- [5] Zálán Borsos, Mojmir Mutny, and Andreas Krause. Coresets via bilevel optimization for continual learning and streaming. *Advances in Neural Information Processing Systems*, 33:14879–14890, 2020. 2
- [6] Francisco M Castro, Manuel J Marín-Jiménez, Nicolás Guil, Cordelia Schmid, and Karteek Alahari. End-to-end incremental learning. In *Proceedings of the European conference on computer vision (ECCV)*, pages 233–248, 2018. 1, 2, 7, 8
- [7] George Cazenavette, Tongzhou Wang, Antonio Torralba, Alexei A Efros, and Jun-Yan Zhu. Dataset distillation by matching training trajectories. In *Proceedings of the IEEE/CVF Conference on Computer Vision and Pattern Recognition*, pages 4750–4759, 2022. 1, 3, 5, 6, 7, 8
- [8] Yutian Chen, Max Welling, and Alex Smola. Super-samples from kernel herding. *arXiv preprint arXiv:1203.3472*, 2012. 6
- [9] Zhiwei Deng and Olga Russakovsky. Remember the past: Distilling datasets into addressable memories for neural networks. *arXiv preprint arXiv:2206.02916*, 2022. 3
- [10] Jacob Devlin, Ming-Wei Chang, Kenton Lee, and Kristina Toutanova. Bert: Pre-training of deep bidirectional transformers for language understanding. *arXiv preprint arXiv:1810.04805*, 2018. 1
- [11] Alexey Dosovitskiy, Lucas Beyer, Alexander Kolesnikov, Dirk Weissenborn, Xiaohua Zhai, Thomas Unterthiner, Mostafa Dehghani, Matthias Minderer, Georg Heigold, Sylvain Gelly, et al. An image is worth 16x16 words: Transformers for image recognition at scale. *arXiv preprint arXiv:2010.11929*, 2020. 1
- [12] Jiawei Du, Yidi Jiang, Vincent TF Tan, Joey Tianyi Zhou, and Haizhou Li. Minimizing the accumulated trajectory error to improve dataset distillation. *arXiv preprint arXiv:2211.11004*, 2022. 3
- [13] Yilun Du, Shuang Li, Joshua Tenenbaum, and Igor Mordatch. Improved contrastive divergence training of energy based models. *arXiv preprint arXiv:2012.01316*, 2020. 4
- [14] Yilun Du and Igor Mordatch. Implicit generation and modeling with energy based models. *Advances in Neural Information Processing Systems*, 32, 2019. 4, 5
- [15] Reza Zanjirani Farahani and Masoud Hekmatfar. *Facility location: concepts, models, algorithms and case studies*. Springer Science & Business Media, 2009. 1, 2, 7, 8
- [16] Chelsea Finn, Pieter Abbeel, and Sergey Levine. Model-agnostic meta-learning for fast adaptation of deep networks. In *International conference on machine learning*, pages 1126–1135. PMLR, 2017. 3
- [17] Cong Geng, Jia Wang, Zhiyong Gao, Jes Frellsen, and Søren Hauberg. Bounds all around: training energy-based models with bidirectional bounds. *Advances in Neural Information Processing Systems*, 34:19808–19821, 2021. 4
- [18] Kaiming He, Xiangyu Zhang, Shaoqing Ren, and Jian Sun. Deep residual learning for image recognition. In *Proceedings of the IEEE conference on computer vision and pattern recognition*, pages 770–778, 2016. 1
- [19] Kaiming He, Xiangyu Zhang, Shaoqing Ren, and Jian Sun. Deep residual learning for image recognition. In *Proceedings of the IEEE conference on computer vision and pattern recognition*, pages 770–778, 2016. 7, 8
- [20] Geoffrey E Hinton. Training products of experts by minimizing contrastive divergence. *Neural computation*, 14(8):1771–1800, 2002. 4
- [21] Arthur Jacot, Franck Gabriel, and Clément Hongler. Neural tangent kernel: Convergence and generalization in neural networks. *Advances in neural information processing systems*, 31, 2018. 3
- [22] Zixuan Jiang, Jiaqi Gu, Mingjie Liu, and David Z Pan. Delving into effective gradient matching for dataset condensation. *arXiv preprint arXiv:2208.00311*, 2022. 3
- [23] Mohammad Emtiyaz Khan and Håvard Rue. The bayesian learning rule. *arXiv preprint arXiv:2107.04562*, 2021. 3
- [24] Krishnateja Killamsetty, Guttu Sai Abhishek, Alexandre V Evfimievski, Lucian Popa, Ganesh Ramakrishnan, Rishabh Iyer, et al. Automata: Gradient based data subset selection for compute-efficient hyper-parameter tuning. *arXiv preprint arXiv:2203.08212*, 2022. 1, 2
- [25] Balhae Kim, Jungwon Choi, Seanie Lee, Yoonho Lee, Jungwoo Ha, and Juho Lee. On divergence measures for bayesian pseudocoresets. *arXiv preprint arXiv:2210.06205*, 2022. 2, 3, 4, 6, 7, 8
- [26] Jang-Hyun Kim, Jinuk Kim, Seong Joon Oh, Sangdoo Yun, Hwanjun Song, Joonhyun Jeong, Jungwoo Ha, and Hyun Oh Song. Dataset condensation via efficient synthetic-data parameterization. In *International Conference on Machine Learning*, pages 11102–11118. PMLR, 2022. 2
- [27] Suraj Kothawade, Atharv Savarkar, Venkat Iyer, Ganesh Ramakrishnan, and Rishabh Iyer. Clinical: Targeted active learning for imbalanced medical image classification. In *Medical Image Learning with Limited and Noisy Data: First International Workshop, MILLanD 2022, Held in Conjunction with MICCAI 2022, Singapore, September 22, 2022, Proceedings*, pages 119–129. Springer, 2022. 2
- [28] Alex Krizhevsky, Geoffrey Hinton, et al. Learning multiple layers of features from tiny images. 2009. 6
- [29] Alex Krizhevsky, Ilya Sutskever, and Geoffrey E Hinton. Imagenet classification with deep convolutional neural networks. *Communications of the ACM*, 60(6):84–90, 2017. 1

- [30] Alex Krizhevsky, Ilya Sutskever, and Geoffrey E Hinton. Imagenet classification with deep convolutional neural networks. *Communications of the ACM*, 60(6):84–90, 2017. 7, 8
- [31] Ya Le and Xuan Yang. Tiny imagenet visual recognition challenge. *CS 231N*, 7(7):3, 2015. 6
- [32] Yann LeCun, Léon Bottou, Yoshua Bengio, and Patrick Haffner. Gradient-based learning applied to document recognition. *Proceedings of the IEEE*, 86(11):2278–2324, 1998. 6
- [33] Saehyung Lee, Sanghyuk Chun, Sangwon Jung, Sangdo Yun, and Sungroh Yoon. Dataset condensation with contrastive signals. In *International Conference on Machine Learning*, pages 12352–12364. PMLR, 2022. 3
- [34] Guang Li, Ren Togo, Takahiro Ogawa, and Miki Haseyama. Dataset distillation using parameter pruning. *arXiv preprint arXiv:2209.14609*, 2022. 3
- [35] Noel Loo, Ramin Hasani, Alexander Amini, and Daniela Rus. Efficient dataset distillation using random feature approximation. *arXiv preprint arXiv:2210.12067*, 2022. 3
- [36] Dionysis Manousakas, Zuheng Xu, Cecilia Mascolo, and Trevor Campbell. Bayesian pseudocoresets. *Advances in Neural Information Processing Systems*, 33:14950–14960, 2020. 1, 3, 4, 6, 7, 8
- [37] Timothy Nguyen, Zhourong Chen, and Jaehoon Lee. Dataset meta-learning from kernel ridge-regression. In *International Conference on Learning Representations*, 2021. 1, 3, 6, 7, 8
- [38] Alec Radford, Jong Wook Kim, Chris Hallacy, Aditya Ramesh, Gabriel Goh, Sandhini Agarwal, Girish Sastry, Amanda Askell, Pamela Mishkin, Jack Clark, et al. Learning transferable visual models from natural language supervision. In *International conference on machine learning*, pages 8748–8763. PMLR, 2021. 1
- [39] Sylvestre-Alvise Rebuffi, Alexander Kolesnikov, Georg Sperl, and Christoph H Lampert. icarl: Incremental classifier and representation learning. In *Proceedings of the IEEE conference on Computer Vision and Pattern Recognition*, pages 2001–2010, 2017. 1, 2
- [40] Ozan Sener and Silvio Savarese. Active learning for convolutional neural networks: A core-set approach. *arXiv preprint arXiv:1708.00489*, 2017. 1, 2, 7, 8
- [41] Pierre Sermanet, Soumith Chintala, and Yann LeCun. Convolutional neural networks applied to house numbers digit classification. In *Proceedings of the 21st international conference on pattern recognition (ICPR2012)*, pages 3288–3291. IEEE, 2012. 6
- [42] Karen Simonyan and Andrew Zisserman. Very deep convolutional networks for large-scale image recognition. *arXiv preprint arXiv:1409.1556*, 2014. 7, 8
- [43] Samarth Sinha, Han Zhang, Anirudh Goyal, Yoshua Bengio, Hugo Larochelle, and Augustus Odena. Small-gan: Speeding up gan training using core-sets. In *International Conference on Machine Learning*, pages 9005–9015. PMLR, 2020. 2
- [44] Mariya Toneva, Alessandro Sordoni, Remi Tachet des Combes, Adam Trischler, Yoshua Bengio, and Geoffrey J Gordon. An empirical study of example forgetting during deep neural network learning. *arXiv preprint arXiv:1812.05159*, 2018. 2, 6, 7, 8
- [45] Kai Wang, Bo Zhao, Xiangyu Peng, Zheng Zhu, Shuo Yang, Shuo Wang, Guan Huang, Hakan Bilen, Xinchao Wang, and Yang You. Cafe: Learning to condense dataset by aligning features. In *Proceedings of the IEEE/CVF Conference on Computer Vision and Pattern Recognition*, pages 12196–12205, 2022. 1, 3, 6, 7, 8
- [46] Tongzhou Wang, Jun-Yan Zhu, Antonio Torralba, and Alexei A Efros. Dataset distillation. *arXiv preprint arXiv:1811.10959*, 2018. 2, 3, 6, 7
- [47] Max Welling. Herding dynamical weights to learn. In *Proceedings of the 26th Annual International Conference on Machine Learning*, pages 1121–1128, 2009. 1, 2, 7, 8
- [48] Han Xiao, Kashif Rasul, and Roland Vollgraf. Fashion-mnist: a novel image dataset for benchmarking machine learning algorithms. *arXiv preprint arXiv:1708.07747*, 2017. 6
- [49] Ruonan Yu, Songhua Liu, and Xinchao Wang. Dataset distillation: A comprehensive review. *arXiv preprint arXiv:2301.07014*, 2023. 3
- [50] Bo Zhao and Hakan Bilen. Dataset condensation with differentiable siamese augmentation. In *International Conference on Machine Learning*, pages 12674–12685. PMLR, 2021. 1, 3, 6, 7, 8
- [51] Bo Zhao and Hakan Bilen. Synthesizing informative training samples with gan. *arXiv preprint arXiv:2204.07513*, 2022. 3
- [52] Bo Zhao and Hakan Bilen. Dataset condensation with distribution matching. In *Proceedings of the IEEE/CVF Winter Conference on Applications of Computer Vision*, pages 6514–6523, 2023. 1, 3, 6, 7, 8
- [53] Bo Zhao, Konda Reddy Mopuri, and Hakan Bilen. Dataset condensation with gradient matching. In *International Conference on Learning Representations*, 2021. 1, 2, 3, 6, 7, 8
- [54] Yongchao Zhou, Ehsan Nezhadarya, and Jimmy Ba. Dataset distillation using neural feature regression. In Alice H. Oh, Alekh Agarwal, Danielle Belgrave, and Kyunghyun Cho, editors, *Advances in Neural Information Processing Systems*, 2022. 1, 3